

Fast CXRS-Measurements in the Edge Transport Barrier of ASDEX Upgrade

T. Pütterich, C.F. Maggi, L.D. Horton, R. Dux,
B. Langer, E. Wolfrum and the ASDEX Upgrade Team

Max-Planck-Institut für Plasmaphysik, EURATOM Assoc., D-85748 Garching, Germany

In H-mode plasmas the turbulent transport of energy and particles is strongly suppressed in a thin radial region at the edge of the confined plasma. The width of this edge transport barrier (ETB) is rather small (for ASDEX Upgrade about 2cm) with large radial gradients for T_e , T_i and n_e . For ELMy H-modes, edge-localized modes (ELMs) occur which make the steep gradients of electron temperature and density collapse for a few 100 microseconds. These recover again in the following milliseconds until the next ELM occurs. The details of this barrier determine how well the plasma confines energy enhancing its performance and how well it confines impurities and He ash which, in general, reduces the performance of a fusion plasma. The small spatial extent of the barrier and the fast change due to ELMs requires a diagnostic with good spatial and temporal resolution.

New CXRS Diagnostic Focussed on the Plasma Pedestal

A new diagnostic based on charge-exchange recombination spectroscopy (CXRS) at one of the heating beams has been designed with the aim to investigate the plasma edge in H-mode discharges. An in-vessel optical setup images the ETB region onto several optical fibres with 400 μm core diameter. To collect additional light, each of the 8 lines-of-sight (LOS) is equipped with 3 optical fibres. The light of the fibres is dispersed by a high-throughput spectrometer ($f/4$, $f=280$ mm) which facilitates two commercial objective lenses with very good imaging properties. A frame-transfer CCD with 512x512 pixels and electron-multiplying read-out is used to detect the spectra of up to 15 channels (a subset of the 24 fibres) with a repetition time of 1.9 ms. High spatial resolution can only be achieved in toroidal viewing geometry. The resolution (in the range of 5 mm) is limited by the curvature of the plasma (large radius at outer midplane ≈ 2.15 m) within the heating beam width (≈ 0.2 m). It was necessary to use a separate mirror for each LOS not to compromise spatial resolution. In an iterative approach of adjusting and measuring the LOS were brought close to the optimal position, which has been found by a 3D computer model which determined the spatial extent of the emitting volumes for each LOS.

CX spectra of NeX, CVI and HeII

The quality of the measured data allows for very short exposure times. In the following, all measurements have been performed with 1.9 ms repetition time. In figure 1, example spectra are presented for NeX, CVI and HeII spectral lines along with spectral fits including background and passive components if applicable. The NeX line is fitted with a single gaussian, since the passive component is very small. For the presented CVI line at the pedestal-top, the passive component is about a factor of 5-20 weaker than the active line, and a two-gaussian fit is used to describe the spectra for all LOS. It may be noted that a passive CX line (CX with background hydrogen) does not play an important role in the spectrum. For the HeII line at the pedestal-top, the active CX-line is about a factor of 2-3 more intense than the passive, and a two gaussian fit is used. However, as the viewing geometry is mainly in toroidal direction the so-called plume effect [1] needs to be taken into account when interpreting the measurements of the presented HeII line. In the following the focus is put on the CVI line.

Analyses of ETB Transport

The C^{6+} -densities are calculated from intensities of the active CX component. To this end, the local densities of the 3 energy components of the deuterium heating beam operated at an acceleration voltage of ≈ 60 kV are taken into account. The attenuation as well as the excitation of beam neutrals is calculated along the path of the beam. This is accomplished using CX rates and atomic data for hydrogen from the ADAS Project [2]. The excited fraction of the hydrogen beam is calculated time-dependently to correct for non-equilibrium effects which occur when the beam neutrals pass the regions with steep gradients of the density and temperature profiles. Figure 2 shows the resulting C^{6+} -density profiles versus the normalized poloidal flux label ρ_{pol} from a discharge phase (#22273 3.2 – 3.5 s) with constant ELM-frequency (63 Hz). The data are sorted according to the time distance to an ELM. During the considered phase, the plasma position was shifted by about 2 cm, such that all plasma diagnostics provide best edge data. Other parameters of the discharge are $I_p = 1$ MA, $B_t = -2.5$ T, $q_{95} = 4.5$, $P_{aux} = 2.5$ MW, $n_e/n_{GW} = 0.65$. The distance between $\rho_{pol} = 0.98$ and 1.00 equals about 1 cm radial distance in the outer midplane of ASDEX Upgrade. In figure 3, measured and fitted electron profiles of the considered discharge phase are presented. The uncertainty of the separatrix position from magnetic reconstruction can be

greatly reduced with the help of the steep T_e -profiles by setting $T_{e,sep} = 100$ eV, a mandatory condition set by the parallel heat transport and power balance [3]. The n_e -profiles from the Li-beam are then aligned to the measurements of the Thomson scattering, as for the latter diagnostic the measurement volumes

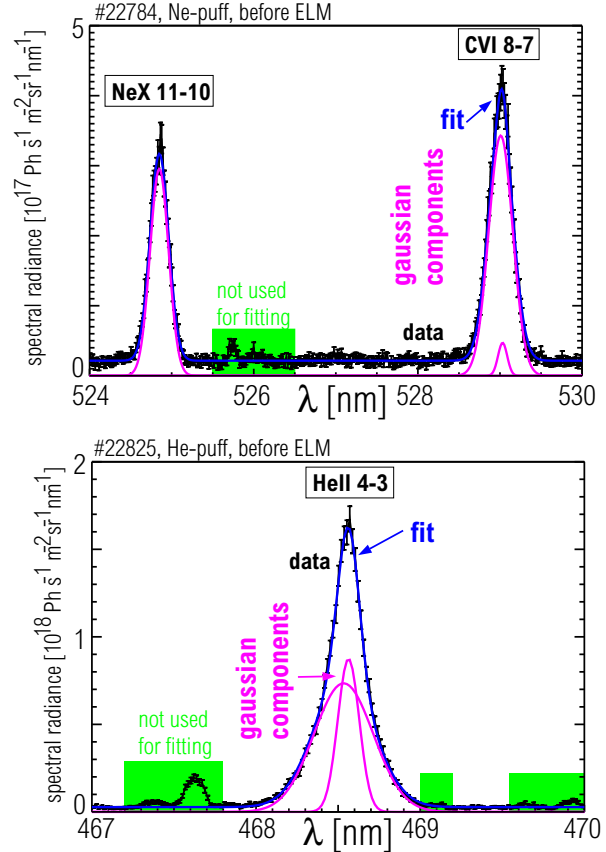


Fig. 1: Example spectra are presented for NeX, CVI and HeII spectral lines along with spectral fits. Repetition time: 1.9 ms - above spectra are taken before the occurrence of an ELM ($f_{ELM} \approx 100$ Hz).

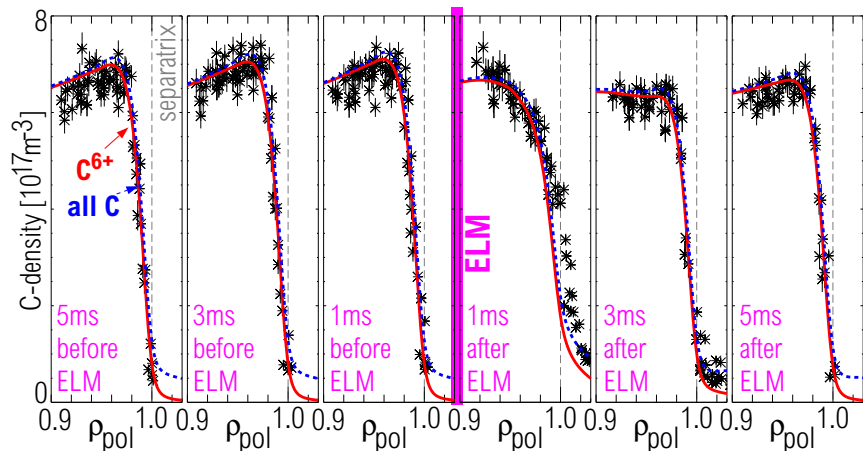


Fig. 2: Result of an ELM-synchronized data analysis. A time sequence around a single ELM is presented along with the results from the transport model (lines, details see below).

are identical for electron temperatures and densities. The CX-data are then aligned with an accuracy of about 2-3 mm, such that the steep T_i -gradient region coincides with that of the T_e -measurement (see figure 3). The necessary corrections are typically smaller than 5 mm.

The evolution of the C^{6+} -density profiles was modelled with the impurity transport code STRAHL [4,5], which takes into account ionization and recombination rates and calculates time-dependently the densities of all ionization stages along the plasma radius in a flux surface averaged manner. The local ionization and recombination rates are evaluated by taking the measured electron profiles into account. The impurity transport is treated using a flux surface averaged diffusion coefficient (D) and drift velocity (v) profile. In the actual case, 200 ELM cycles were simulated, while a constant carbon (neutral C) influx was assumed. After the simulated 200 ELM cycles the C-density has arrived definitely at a quasi-equilibrium, which is modulated by the ELMs. The quasi-equilibrium depends on the transport coefficients and the chosen C-influx. In the model, the effects of an ELM are imitated by increasing D ($10 \text{ m}^2/\text{s}$) for $200 \mu\text{s}$ at the pedestal region, while the transport in-between ELMs is subject of this investigation. It is known from earlier reports (e.g. [7]) that

the transport barrier in an H-mode plasma is located at the very edge of the plasma, while just inside that barrier a relatively large turbulent (diffusive) transport is found (in the range of $1 \text{ m}^2/\text{s}$). For the actual case, a slightly hollow C^{6+} -density profile is found inside $\rho_{pol} = 0.96$, which is adjusted by assuming a moderate inward pinch of 1 m/s . However, the model aims to find the transport coefficients in the barrier itself by assuming a decrease of the diffusion coefficient and by assuming a local drift velocity at the barrier. The steep gradients in the C^{6+} -density just before the occurrence of an ELM can only be achieved with an inward drift. Local ratios of v/D at $\rho_{pol} = 0.99$ are fitted to be $-80 \pm 20 \text{ m}^{-1}$ nearly independent of other model assumptions. For the radial location of these steep gradients the absolute values of v are important and can be obtained. This is done by a least square fit for which the D and v profiles have been modified by a gaussian-like disturbance in the barrier region. The width, location and amplitude of these disturbances were determined by the fit in which only the relative shape of the C^{6+} -density profile between $\rho_{pol} = 0.96$ and $\rho_{pol} = 1.03$ was considered. The best agreement (s. model curves in figure 2) is found for the transport coefficients depicted in figure 4 (black, solid). Evaluating the uncertainties of the fit-parameters, the diffusion coefficient is found to be in the range $0.1\text{-}0.4 \text{ m}^2/\text{s}$ at $\rho_{pol} = 0.99$. The transport coefficients in the ETB (compared at $\rho_{pol} = 0.99$) are in agreement with neoclassical predictions for impurity transport (D_{neo} and v_{neo}) taken from the code NEOART [5,6]. It may be noted, that the neo-

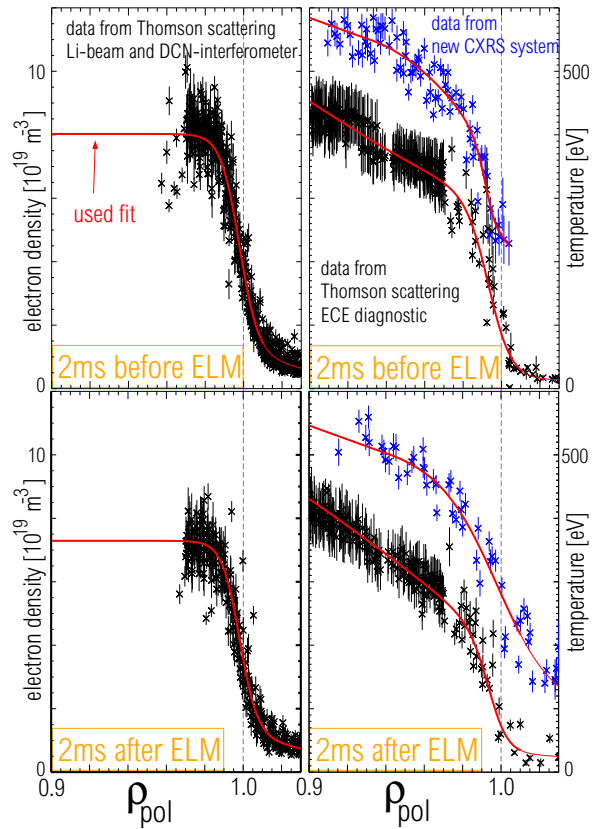


Fig. 3: Temperature and density profiles before and after an ELM as measured during the analysed discharge phase.

classical prediction for the D exhibits different shape along ρ_{pol} than the used model function, but the latter is supposed to take also the turbulent transport inside the edge barrier into account. From basic transport considerations follows that the increase of C-density from separatrix to $\rho_{pol} = 0.97$ can be calculated by integrating the ratio v/D , such that:

$$F = \frac{n_C(\rho_{pol} = 0.97)}{n_C(\rho_{pol} = 1.0)} = \exp\left[\int_{\rho_{pol}=1.0}^{\rho_{pol}=0.97} \frac{v}{D} dr\right]$$

For the present evaluation, $F = 6.1$ which is comparable to the findings for Ne in [7,8]. For illustrating this ratio, the C-density profile is also depicted in figure 2 (dashed, blue) as calculated by the transport model. Two sources of uncertainty for the analysis have been investigated. Firstly, the carbon source in the experiment is time dependent. Secondly, the effect of the ELM is only imitated in the model by an increased diffusion coefficient. To investigate these effects, the carbon source has been increased after an ELM (different values and timings have been tested), and the removal of carbon from the plasma was varied, using different values for the diffusion coefficients during an ELM. Additionally, a strong variation of the parallel loss time of the impurities in the SOL towards the divertor was tested. Both investigations prove that the steep gradient of the C^{6+} -density at the ETB is rather insensitive to such variations and depends mainly on the local value of v/D . It seems possible, that the discussed uncertainties are responsible for the small discrepancy in the gradient position between the model and the measurements just after an ELM (1ms after ELM, figure 2). The latter might also be the effect of the plasma movement due to the ELM. This movement is corrected for, but possibly a discrepancy of few mm remains.

References

- [1] R. J. Fonck *et al.*, Physical Review A **29**, 3288 (1984).
- [2] H. P. Summers, The ADAS User Manual, version 2.6 <http://adas.phys.strath.ac.uk> (2004)
- [3] J. Neuhauser *et al.*, PPCF **44**, 855 (2002).
- [4] K. Behringer, JET-R(87)08, JET Joint Undertaking, Culham (1987)
- [5] R. Dux, Technical Report No. 10/30, IPP, Garching, Germany (2006)
- [6] A. G. Peeters, provided the NEOART code (1998)
- [7] R. Dux, Fusion Science and Technology **44**, 708 (2003)
- [8] A. Kallenbach *et al.*, Proc. of the 24th EPS Conference on Controlled Fusion and Plasma Physics, Berchtesgaden, 1997, Vol. 21A, part IV, pp. 1473–1476.

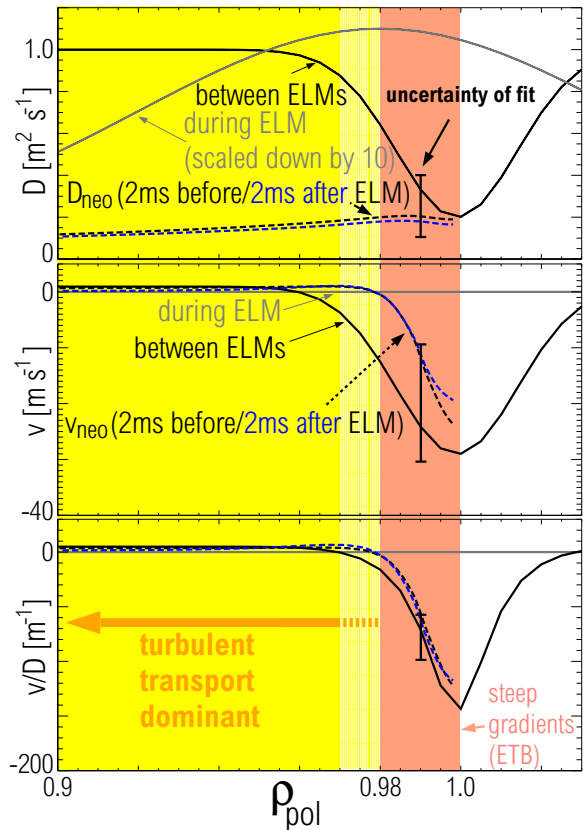


Fig. 4: Transport coefficients obtained by the presented analysis are compared to neoclassical transport coefficients. Due to the additional turbulent transport the comparison is relevant in the ETB region.